Engineering Science and Technology, an International Journal 24 (2021) 1361–1372

HOSTED BY

Contents lists available at ScienceDirect

Engineering Science and Technology, an International Journal

journal homepage: www.elsevier.com/locate/jestch

Durability of preflex beam under cyclic loading

Ahmadullah Nasiri *, Tetsuhiro Shimozato

Department of Civil Engineering and Architecture, Graduate School of Engineering and Science, University of the Ryukyus, Nishihara, Okinawa, Japan

ARTICLE INFO

Article history:
Received 6 November 2020
Revised 14 February 2021
Accepted 2 March 2021
Available online 18 March 2021

Keywords:
Concrete crack width
Cyclic loading
Durability
Preflex beam
Prestress loss

ABSTRACT

Preflex beam girders with remarkable advantages are widely used in bridge structures. With aging, preflex beam bridges undergo concrete cracking and degrade as the cracks propagate and deteriorate due to repeated service load application and exposure to humid and saline environment. The objective of this study was to evaluate concrete cracking, changes in prestress, and consequent changes in sectional properties as the preflex beam undergoes deterioration in its concrete casing under cyclic loading. The experimental study investigated the behavior of a preflex beam specimen under multiple cyclic loading ranges, reproducing different deterioration levels in the concrete casing of the specimen. Relating concrete deterioration to resulting changes in the girder's structural behavior, the study outlined recommendations for monitoring approaches in actual bridges. The study concluded that with advancement in concrete deterioration, the preflex beam girder loses prestress that results in reduced strength of the girder and remarkable changes in its sectional properties. The study also concluded to minimize prestress loss and changes in sectional properties of the girder, closer spacing for shear ribs welded to the lower flange can be helpful.

1. Introduction

Preflex beam is a composite of a welded steel plate girder and reinforced concrete around the steel-lower-flange that is prestressed utilizing the preflex technology. Specified pre-camber in the steel-lower-flange and shear ribs welded to the bottom of the flange are used in this type of composite girders [1,2]. These girders with lower section height and longer span as the main advantages, are well suited for intersections and cross-river bridges.

This type of girders experience degradation as they undergo deterioration in the lower-flange concrete, under repeated application of service loads, and exposure to hazardous elements from humid and saline environments. This in turn leads to changes in structural behavior of composite member resulting in its reduced serviceability. Therefore, understanding the deterioration process of these girders under repeated service load, changes in their structural behavior, and other mechanical properties, is important. Fig. 1 shows a 40 years old preflex beam bridge with cracks in the lower-flange concrete and deterioration due to chloride ion penetration in a humid and severely saline environment.

Degradation of composite members due to concrete cracking mechanisms other than cracking under service load application are also of high importance. Considering concrete unsoundness as another common cracking mechanism, Maruyama et al. [3] investigated soundness assessment procedure for concrete members. The study confirmed degradation of concrete due to aggregate expansion that causes crack formation in concrete leading to reduced compressive strength and young's modulus of the concrete. The study also developed a numerical analysis method to predict physical properties in concrete members and their changes over time. Aiming at evaluation of cement soundness Kabir et al. [4] studied expansive behavior and microstructure of cements having different chemical compositions. The study found autoclave expansion test not to be providing realistic basis for assessing volume stability as well as for rejecting use of portland cement in concrete.

Experimental load rating and analysis of the preflex beam in the construction stage and under test loads studied by Portela et al. [5] can be referred as a detailed approach to understanding behavior of the preflex beam in construction and service stages. Tests conducted by Bae et al. [6] on conventional preflex beams, preflex beams with shear connecters, and preflex beams with shear keys, found that stresses in the preflex beam section from the construction stage can be greater than expected, resulting in loss of camber and tension cracking in concrete.

Watanabe et al. [7] has explained development of segmental prefabrication of preflex beam as an improved method of construction meeting the demand of the bridge industry. Simplified method of determining time-dependent stresses in lower-flange concrete

* Corresponding author.
E-mail addresses: ahmadullah.1415@gmail.com (A. Nasiri), simozato@tec.u-ryukyu.ac.jp (T. Shimozato).

Peer review under responsibility of Karabuk University.

https://doi.org/10.1016/j.jestch.2021.03.003
2215-0986/

Fig. 1. Deteriorated preflex beam bridge.

of preflex beams due to creep and shrinkage, were presented by Morano et al. [8], and investigation of innovative solutions aimed at structural optimization and cost-saving for this type of beams, by Mannini et al. [9], found cost-saving possible and outlined main advantages of the preflex beams.

Wan et al. [10] experimentally studied how bending behavior of the preflex beam was improved by using a corrugated steel web plate. Destructive test of preflex beam by Kiuchi et al. [11], investigation of structural behavior of preflex beam under experimental testing carried out in Errera et al. [12] and Mink et al. [13], and the study by Zhang et al. [14] addressing both static and fatigue behavior of the preflex beam, can be referred as the research carried out on structural behavior of this type of composite girders.

Furthermore, fatigue behavior of the preflex beam under experimental testing was studied by kikuchi et al. [15], while fatigue strength of the shear ribs welded to the steel-lower-flange of these beams was studied by experimental testing in Yasuhiro et al. [16].

However, relevant research addressing the durability of the preflex beam in terms of concrete post cracking behavior and resulting changes in the beam's mechanical properties that can help improve maintenance approaches for real bridges is not sufficient.

This study aims to clarify structural factors effective and important for evaluating deterioration and consequent changes in sectional properties of the preflex beam, and outline recommendations for monitoring approaches for these girders.

The method used for this study is to reproduce the deterioration that occurs in the concrete casing of the actual preflex beam girder and to clarify resulting changes in the sectional properties of the preflex beam.

Deterioration physically displayed in the form of concrete cracking, crack propagation, efflorescence, and spalling, resulting in changes in steel prestress and consequent changes in mechanical properties of the section, are investigated throughout the experimental loading.

2. Experimental methods

2.1. Test specimen

The geometric details of the only specimen used for the experimental study are shown in Fig. 2. The flange and web plates of the steel plate girder were 16 mm and 9 mm thick, respectively. Shear ribs measuring 13 mm × 13 mm × 75 mm (width × height × length) spaced at 250 mm in one half (right half of Fig. 2(a), hereafter referred to as the 250-mm half) of the length and spaced at 500 mm in the other half (left half in Fig. 2(a) hereafter referred to as the 500-mm half), were welded to the bottom of the lower-flange (Fig. 2(c)), aimed at knowing the effect of shear rib spacing on concrete cracking behavior. All shear rib weld joints were fillet welds without any treatment, running all around the rib. Stud bars of 9 mm in diameter were welded to the web plate during fabrication to support the main reinforcement mesh (Fig. 2(b)).

The reinforcement mesh for the concrete casing consisted of 8 deformed longitudinal rebars of 16 mm in diameter placed in two top and bottom rows with an equal number of rebars in each row. Stirrups were made from 10-mm diameter deformed rebars spaced at 125 mm near the supports and 250 mm around the mid-span. A minimum concrete cover of 35 mm was maintained from all sides in the concrete formwork.

2.2. Material properties

The steel used in the fabrication of the specimen was SM490, as per Japanese Industrial Standards (JIS) with the specifications shown in Table 1, as per the mill test report. The yield strength of the steel reinforcement was 295 MPa. Concrete cylinders were cast, and slump and air content tests were conducted on the day of concrete casting. Wet-cured cylinders were compression tested after five days when preflexion loads were removed, seven days when the specimen testing was started, ten days, and twenty-eight days. Table 2 shows test results with averaged values for modulus of elasticity, tensile strength, and compressive strength, experimental values of the slump and air content, and five days design values. Concrete gained design elastic modulus of 22Gpa, and compressive strength of 18Mpa after five days of curing.

To know the fatigue strength of the weld joints connecting the shear ribs to the bottom of steel-lower-flange plate, ten fatigue test coupons with the same shear ribs welded to them were tested under cyclic loading. Coupon specimens with weld joint running all around the shear rib same as the weld joint in preflex beam specimen, and specimens with weld joint only along the length of the shear rib, were tested. The S-N curve in Fig. 3 shows that the shear rib weld joint qualified for FAT100 class fatigue strength as per the requirements of International Institute of Welding (IIW) [17].

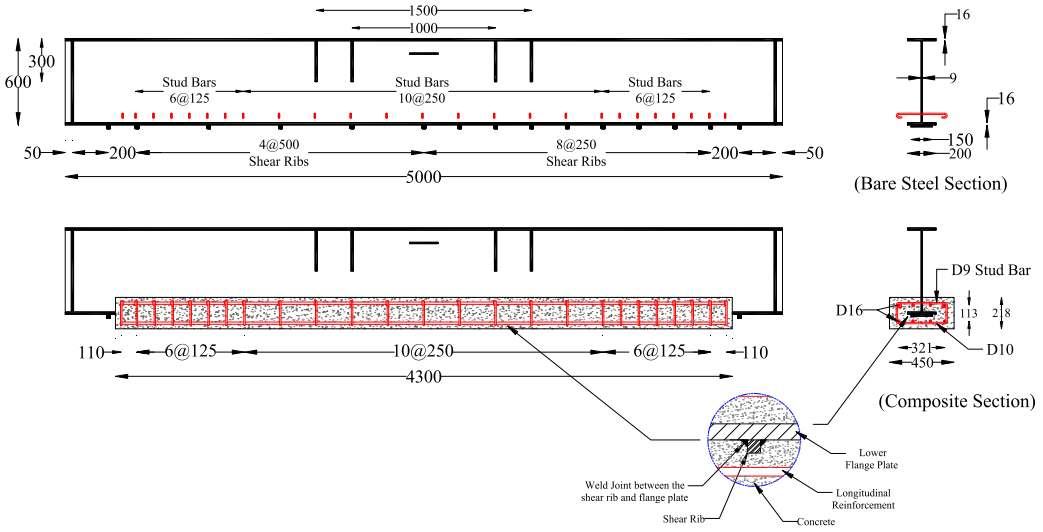

(a) Geometric details of test specimen.

(b) Specimen in experiment laboratory.

(c) Shear rib welded to the lower flange of the specimen.

Fig. 2. Test specimen details.

Table 1
Specifications of steel used in fabrication.

Part	Tensile strength (N/mm^2)		Elongation (%)	Chemical composition (%)				
	Yield	Ultimate		C	Si	Mn	P	S
Flange plate (16 mm)	436	541	25	16	6	153	11	3
Web plate (9 mm)	405	534	24	15	33	139	13	4

Table 2
Concrete mix properties.

Property / Curing period (Days)	5	7	10	28	Required
Modulus of elasticity (GPa)	24.25	26.71	26.23	27.4	22
Compressive strength (MPa)	21.43	24.42	26.2	29.56	18
Tensile strength (MPa)	(2.2–3.0)				
Water-cement ratio	0.66				
Air content (%)	3.4				(3–6)
Slump (cm)	17.5				(15–20)

2.3. Measurement method

Measurement details for the experimental study of the specimen are shown in Fig. 4. Steel strains were measured at the plate girder's height at five sections (A–E) located at the midspan and distances of 250 mm and 1100 mm from the midspan symmetrically on either side of the beam length. Sections A and B were in the 500-mm half, section C was at the midspan, and sections D and E were in the 250-mm half.

Concrete strains were measured in the upper and lower surfaces at five sections symmetrically located from the midspan on one side along the length. The strain in the longitudinal reinforcement bars was also measured at 500 mm from the midspan symmetrically. Deflections were measured by displacement

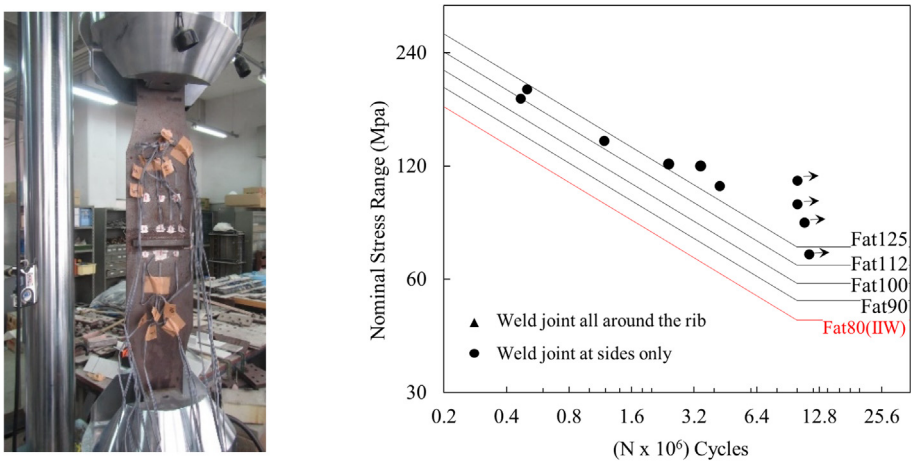

Fig. 3. Fatigue coupon test setup (left) and S-N curve (right).

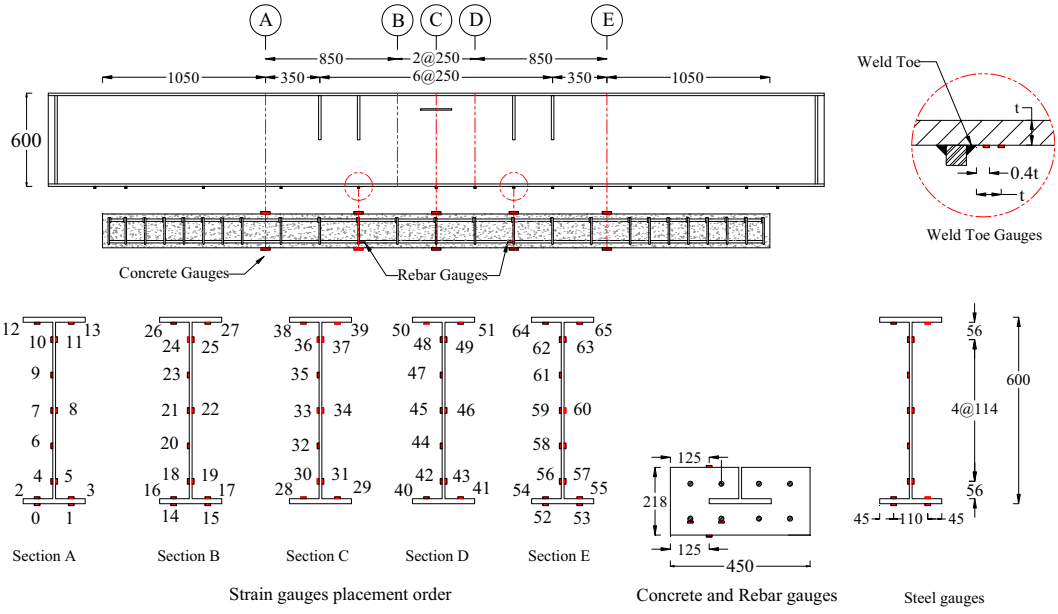

Fig. 4. Measurement details.

transducers at the lower fiber of the composite beam at five points, midspan, 750 mm, and 1500 mm from the center symmetrically on both sides.

2.4. Preflexion method

Preflexion process was carried out using the four-point bending method, as shown in Fig. 5(a). A total of 330 kN was applied using the hydraulic jack, deflecting the specimen to 7.7 mm at the midspan. Subsequently, prestressing concrete (PC) bars with an inner diameter of 32 mm were fixed at the floor level and at the top of the specimen to steel parts laying on the upper flange of the plate girder forming a setup to maintain preflexion (Fig. 5(b)).

Concrete was cast and let cure for five days under this condition. As shown in Fig. 5(c), with the release of preflexion loads, 3.5 mm of midspan deflection recovered while 2.1 mm transformed to compressive prestress in concrete. Under preflexion load, steel lower flange was stressed to 103 MPa at midspan (section C), locating the neutral axis at 333 mm from the bare steel beam's bottom fiber (Fig. 6).

After releasing the preflexion loads, concrete was prestressed to (-1.9 MPa) in the upper surface and (-4.5 MPa) in the lower surface at section C. Steel-lower-flange stresses remaining after release were 61 MPa, 69 MPa, and 61 MPa in sections B, C, and D, respectively. The neutral axis was located at 234 mm from the lower surface of the concrete in section C, at 241 mm in section B, and 236 mm in section D. Changes during testing were monitored referring to these values.

2.5. Experimental program

The testing setup of the specimen under cyclic loading is shown in Fig. 7. To clarify and reproduce deterioration of lower-flange concrete occurring in actual preflex beam girders and changes in their structural properties, experimental loading was carried out in three stages of cyclic loading, each of them being applied in multiple increments, as shown in Fig. 8. The specimen was investigated for changes due to cyclic loading by static tests following cyclic loading increments. The first crack was initiated in section C in the lower surface of concrete at 290 kN with measured concrete

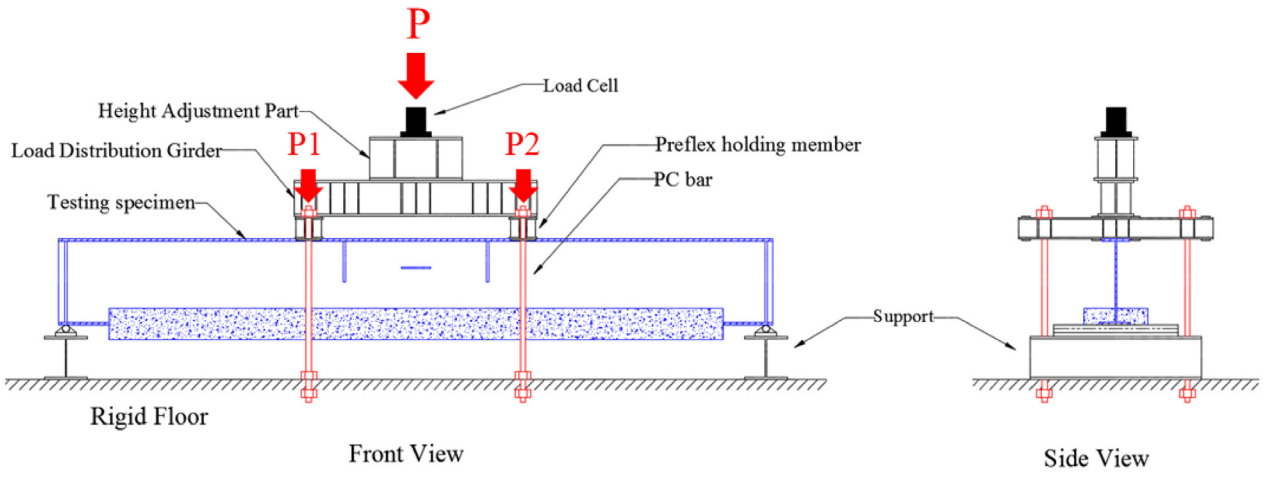

(a) Preflexion method.

(b) Preflexion setup in laboratory.

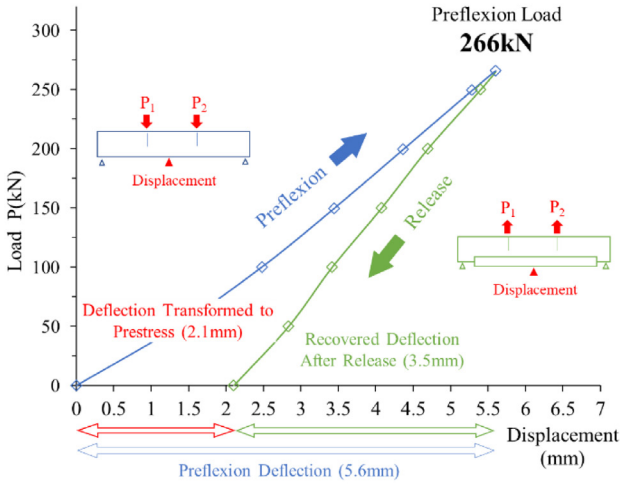

(c) Load and displacement relationship in construction stage.

Fig. 5. Specimen setup details in construction stage.

strain of 94 με (2.44 MPa). Therefore, in stage one the specimen was loaded with load range of 290 kN (10–300 kN) to study the propagation behavior of concrete cracks under cyclic loading, and to monitor consequent changes in sectional properties and prestress. In stage two, under the same load range as in stage one with concrete deterioration advancing under water infiltration into concrete cracks, resulting changes in the specimen's behavior were monitored. In stage three, to study the fatigue performance of steel-lower-flange, the specimen was loaded with a load range of 330 kN (10–340 kN), about 13% larger than the previous stages, developing steel-lower-flange stress ranges meeting Fat100 fatigue class as per IIW [17]. Assuming Fat100 class fatigue strength for shear rib weld joint at steel lower flange, Palmgren-Miner rule [17] was used to estimate the fatigue damage accumulated at the shear rib weld joint in the steel-lower-flange during cyclic loading. Concrete cracking and consequent changes in structural behavior of the specimen were investigated as steel-lower-flange experienced fatigue damage under cyclic loading.

Finally, the specimen was loaded with load cycles developing stress ranges larger than that in stage three to understand how sectional properties change after fatigue crack initiation in the steel-lower-flange.

3. Results

3.1. Stage 1 and stage 2

3.1.1. Concrete crack initiation and propagation

The concrete cracking map and crack details in stage one and stage two of cyclic loadings are shown in Fig. 9, and Fig. 10, respectively. Under static 1.1, crack 1 developed in the concrete's lower surface at the midspan with a length of 350 mm and width smaller than 0.05 mm. Under static 1.2, crack 1 propagated with its width increased to 0.1 mm. Meanwhile, cracks 2 and 3, both with widths smaller than 0.05 mm initiated. By the end of stage one, widths of cracks 2 and 3, increased to 0.05 mm.

In stage two, crack 2 propagated to the upper surface of concrete on either side, and cracks 4–12 developed with widths smaller than 0.05 mm, under static 2.2. Meanwhile, cracks 1 and 3, propagated slightly with no increase in the width. By the end of stage two, crack 2 was the widest crack with a width of 0.25 mm, while cracks 1 and 3, were 0.15 mm and 0.1 mm wide, respectively.

No increase in the length of cracks was seen after static 2.2. Water infiltration into cracks caused spalling and efflorescence in

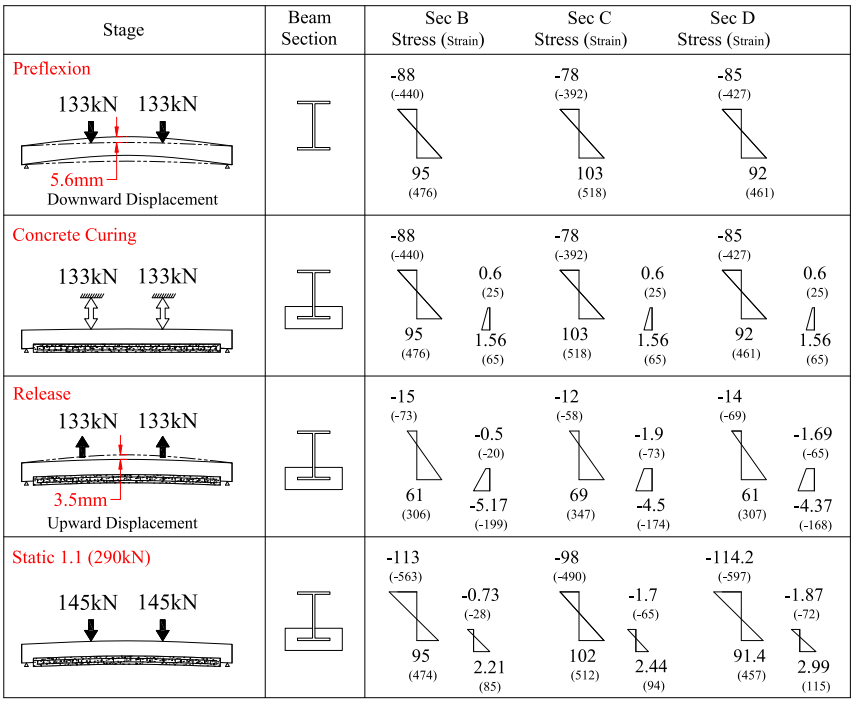

Fig. 6. Stress distribution in the construction and Initial testing stage.

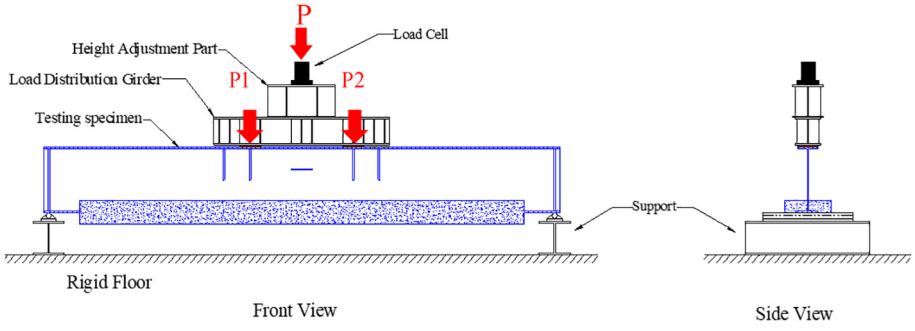

Fig. 7. Loading setup of the specimen.

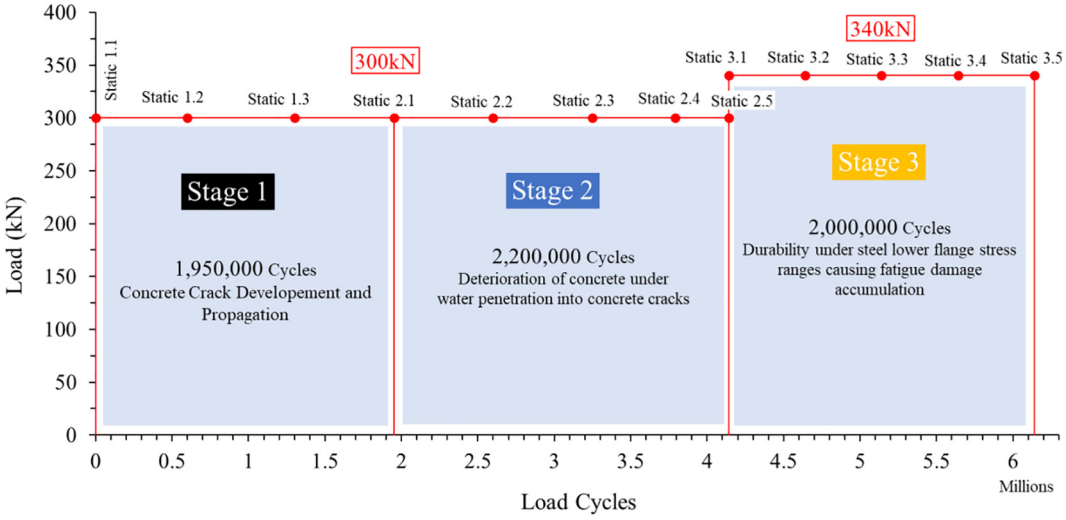

Fig. 8. Experimental program.

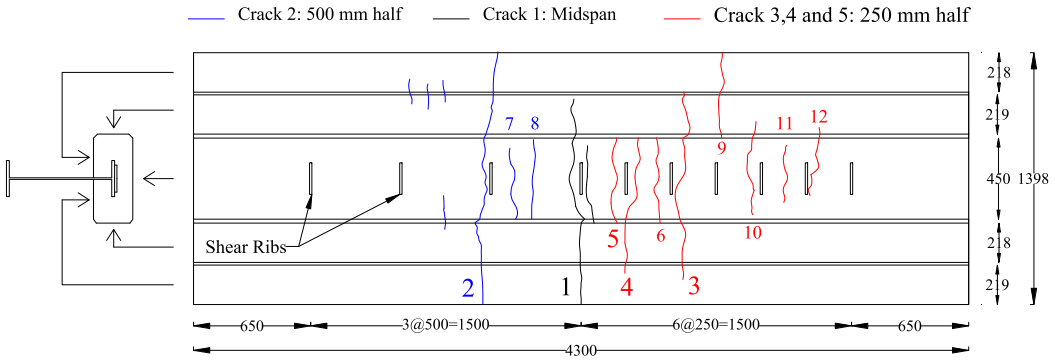

Fig. 9. Concrete crack map in stages 1 and 2.

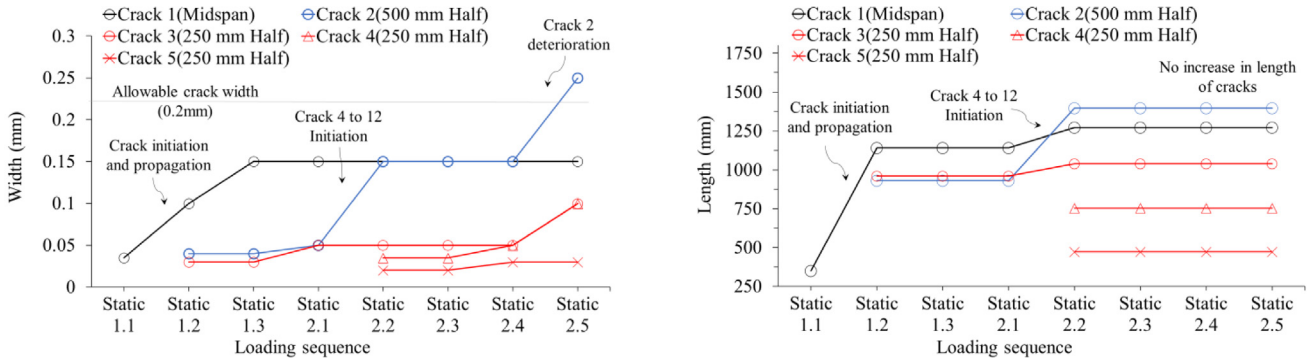

(a) Concrete crack width

(b) Concrete crack length

Fig. 10. Concrete crack details in stages 1 and 2.

concrete cracks, as shown in Fig. 11. Cracks 1–4 experienced efflorescence. However, spalling was seen in cracks 1 and 2 only, being larger in the later, causing an increase in crack width by the end of stage 2.

Cracks developed in the 250-mm half were larger in number but shorter in length, with small crack widths of up to 0.1 mm and slight efflorescence and spalling. However, in the 500-mm half, concrete cracks were fewer but longer, and as wide as 0.25 mm, with severe spalling and efflorescence.

3.1.2. Displacement and neutral axis location

Changes in midspan displacement, and the neutral axis location under cyclic loading are shown in Fig. 12 and Fig. 13, respectively. Initially, with concrete crack 1 with width smaller than 0.05 mm, midspan displacement was 4.15 mm, and neutral axis was located at height (Y_d) of 255 mm in both sections B and D.

Under static 1.2, as width of crack 1 was increased to 0.1 mm, and cracks 2 and 3 were initiated, displacement was increased to 4.46 mm, and neutral axis in sections B and D, raised upward rapidly to 277 mm and 280 mm, respectively. With no remarkable changes in crack widths up to the end of stage one, neutral axis experienced slight changes only in both sections. In stage two, initiation of cracks 4–12 caused changes in neutral axis location and midspan displacement under static 2.2, and this trend continued as water penetration caused further deterioration of concrete, being remarkable in section B.

By the end of stage two, midspan displacement increased to 5 mm, and neutral axis was located at 325 mm in section B in the 500-mm half, while it was located lower at 303 mm in section D in the 250-mm half. Even though cracks were larger in number and as wide as 0.1 mm around section D, but severe efflorescence and spalling, and largest crack width of 0.25 mm in crack 2 in section B, caused remarkable movement of neutral axis in the 500-mm half. Comparing changes in midspan displacement to the changes in neutral axis location, even with concrete crack width advancing to values as large as 0.25 mm, causing remarkable changes in neutral axis location, the reduction rate of stiffness was not remarkable and did not fairly reflect the changes in structural behavior of the girder.

3.1.3. Rebar and steel-lower-flange stress

Rebar stress initially larger in the 250-mm half at 57 MPa than the opposite half at 19 MPa, changed due to concrete deterioration as shown in Fig. 14. Under static 1.2, with the width of crack 1 increased to 0.1 mm and cracks 2 and 3 initiated, rebar stress increased to 116 MPa in the 250-mm half, and to 55 MPa in the opposite half. It took the latter half more load cycles to increase to 121 MPa under static 1.3. Following the same trend, steel-lower-flange nominal stress, as shown in Fig. 15, initially at about 37 MPa in both halves, increased to 48 MPa in the 250-mm half, and 53 MPa in the opposite half under static 1.2, and did not change remarkably thereafter until the end of stage one.

In stage two, initially due to initiation of cracks 4–12 under static 2.1, and later due to severe efflorescence and spalling in the 500-mm half, leading to increase in width of crack 2 to 0.25 mm, rebar stress changed to 171 MPa under static 2.3 prior to the strain gauges going out of use, and steel-lower-flange nominal stress was 81 MPa by the end of stage two.

However, in the 250-mm half, rebar stress was 114 MPa, and steel-lower-flange nominal stress was 52 MPa by the end of stage

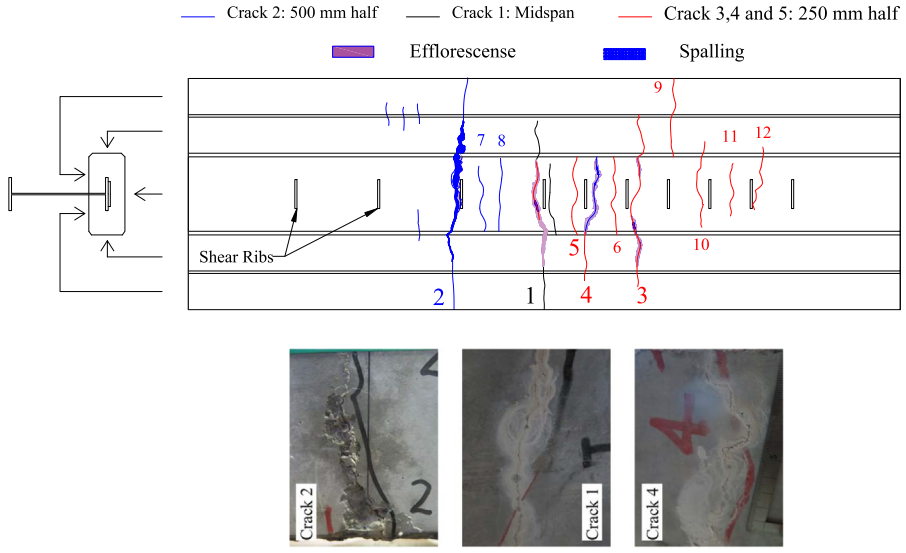

Fig. 11. Efflorescence and spalling in stages 1 and 2.

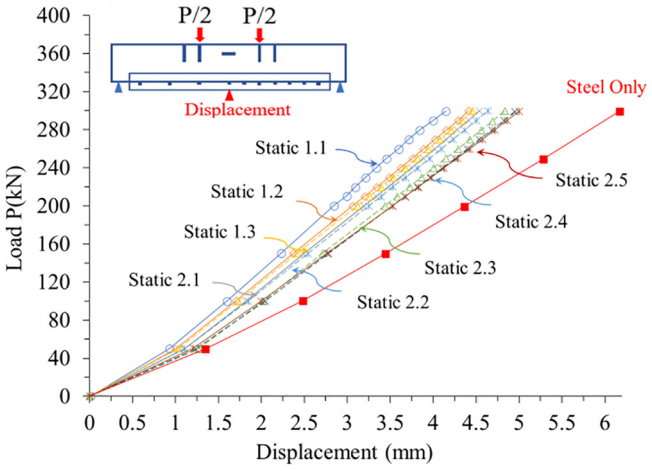

Fig. 12. Load and displacement relationship in stages 1 and 2.

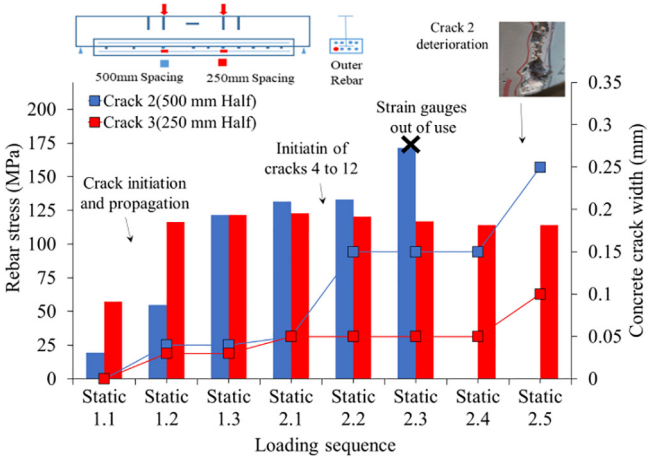

Fig. 14. Rebar stress in stages 1 and 2.

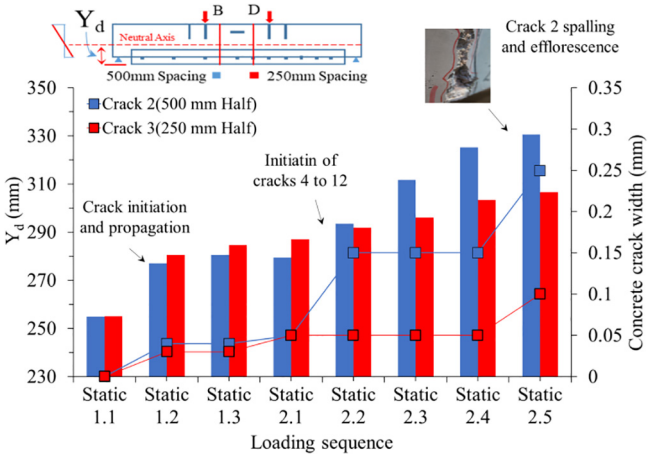

Fig. 13. Neutral axis movement in stages 1 and 2.

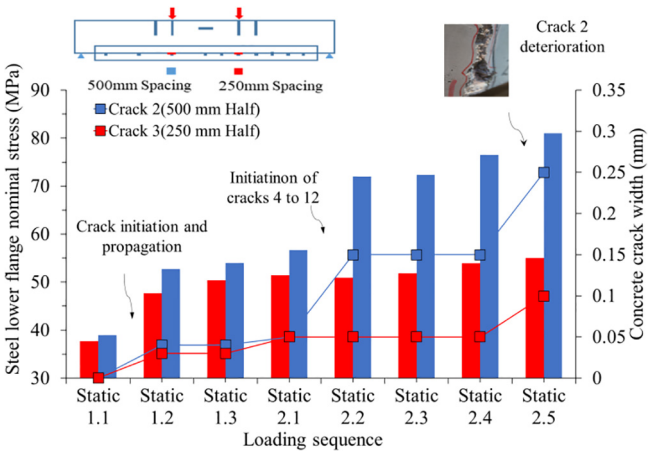

Fig. 15. Steel lower flange nominal stress in stages 1 and 2.

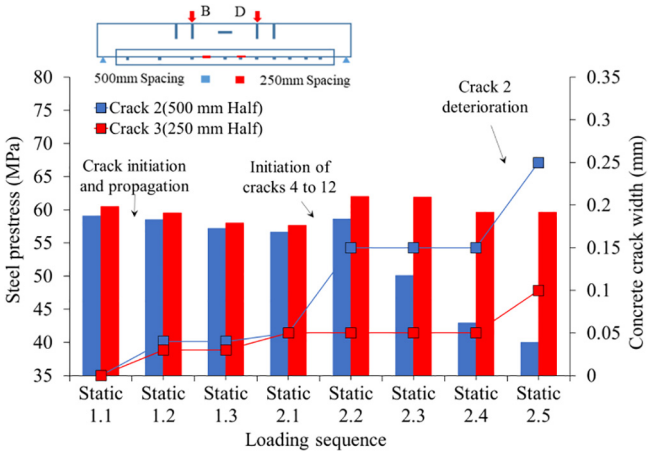

Fig. 16. Steel lower flange prestress in stages 1 and 2.

two with no remarkable change as the width of crack 3 in this half was only 0.1 mm.

3.1.4. Steel-lower-flange prestress

Changes in prestress in steel-lower-flange in sections B and D are shown in Fig. 16. In stage one, with the largest concrete crack width of 0.1 mm (crack 1), steel prestress initially at about 60 MPa in both sections B and D, decreased by 3 MPa only in each section.

In stage two, as the width of concrete crack 2 in the 500-mm half increased to 0.15 mm under static 2.2, steel prestress decreased to 50 MPa in this half and continued to further decrease to 40 MPa by the end of this stage where concrete crack 2 was 0.25 mm wide, with remarkable efflorescence and spalling. However, in the 250-mm half, steel prestress remained almost unchanged as crack 3 in this half was only 0.1 mm wide and did not go through remarkable spalling and efflorescence. Performance of the opposite halves of the length suggest that changes in the steel-lower-flange prestress can very well be related to the advancement of concrete cracking.

The relationship between concrete crack width and loss of steel lower flange prestress is clearly understandable. With an increase in concrete crack width, steel-lower-flange prestress is decreased, consequently causing changes in sectional properties, as shown in Figs. 14–16, leading to reduced stiffness of the section. It is therefore noted that crack width is important and effective as a structural index that can be utilized in monitoring approaches to estimate changes born by the preflex beam.

3.2. Stage 3

3.2.1. Concrete crack propagation

In stage three, since concrete already developed many cracks in previous stages, neither new crack initiations nor propagation of the existing cracks occurred. All cracks remained with the same width throughout stage three except for the crack 2 in the 500-mm half which was 0.3 mm wide under static 3.5. Concrete crack details in this stage are shown in Fig. 17.

3.2.2. Displacement and neutral axis location

The load and displacement relationship under cyclic loading in stage three is shown in Fig. 18. Midspan displacement gradually increased from 5.6 mm under static 3.1, to 6.14 mm under static 3.5. Changes in midspan displacement were slight up to static 3.4. However, change was more visible under static 3.5, where the width of crack 2 increased to 0.3 mm.

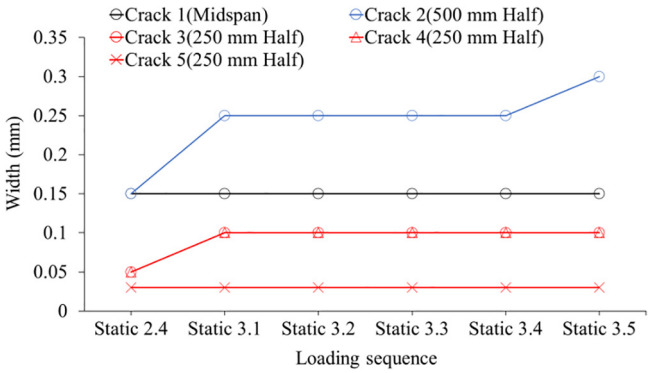

Fig. 17. Concrete crack width in stage 3.

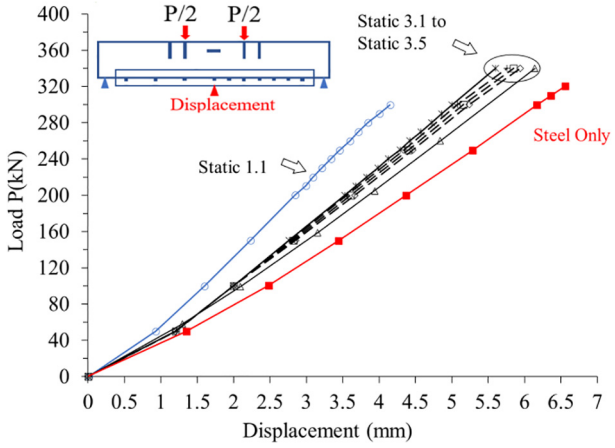

Fig. 18. Load and displacement relationship in stage 3.

Neutral axis, located at 330 mm and 306 mm in sections B and D, respectively, as shown in Fig. 19, moved upward with the rate of change being larger in section D until it was located at the same height at 357 mm in both sections under static 3.5.

Even though no changes were seen on the surface, but concrete cracks got deeper under repeated cyclic loading in stage three. Therefore, a larger number of cracks in the 250-mm half led to a higher rate of change in neutral axis location in this half.

3.2.3. Steel-lower-flange stress

Steel nominal stress range in lower-flange shear rib initially at 87 MPa and 59 MPa, in the 500-mm half and the 250-mm half, respectively, increased steadily up to 92 MPa and 66 MPa, under static 3.4. Under static 3.5, when the width of crack 2 increased to 0.3 mm, stress values changed with a higher rate of change to 102 MPa and 72 MPa, respectively, as shown in Fig. 20.

Steel nominal stress ranges born in the shear rib weld joint of the 500-mm half exceeding the Fat100 class stress range and causing accumulative fatigue damage of 1.01 (Miner Rule) after two million cycles in stage three, confirmed qualification of the steel-lower-flange shear rib weld joints for the Fat100 class fatigue strength, same as the fatigue coupon test results in Fig. 3.

The smaller width of concrete crack at 0.1 mm in the 250-mm half kept steel-lower-flange nominal stress remarkably smaller than the 500-mm half with 0.3 mm concrete crack width.

3.2.4. Steel-lower-flange prestress

Changes in the steel-lower-flange prestress in stage three of cyclic loading are shown in Fig. 21. Initially, at 60 MPa in section

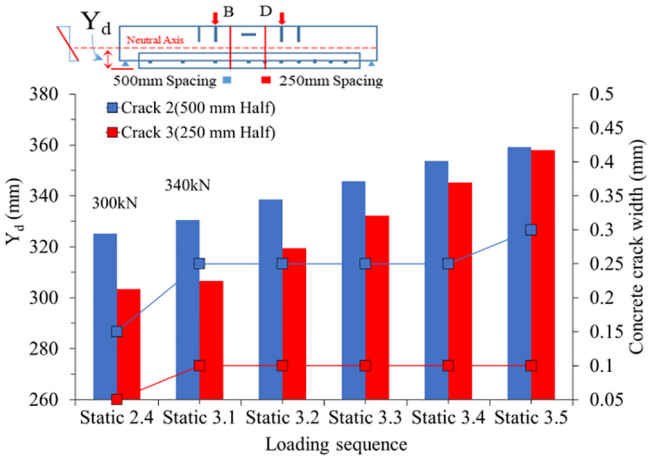

Fig. 19. Neutral axis movement in stage 3.

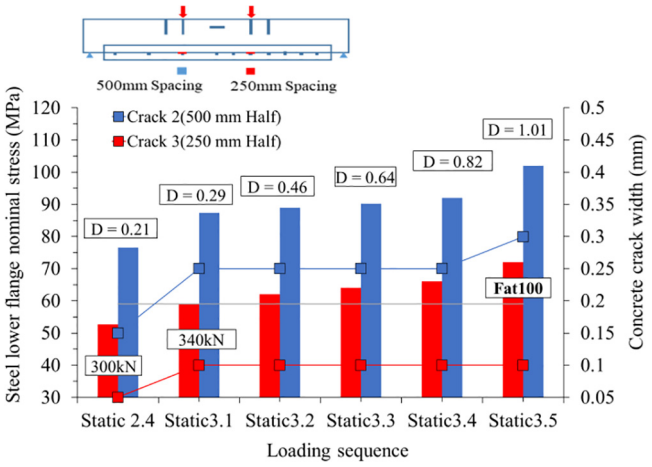

Fig. 20. Steel lower flange nominal stress in stage 3.

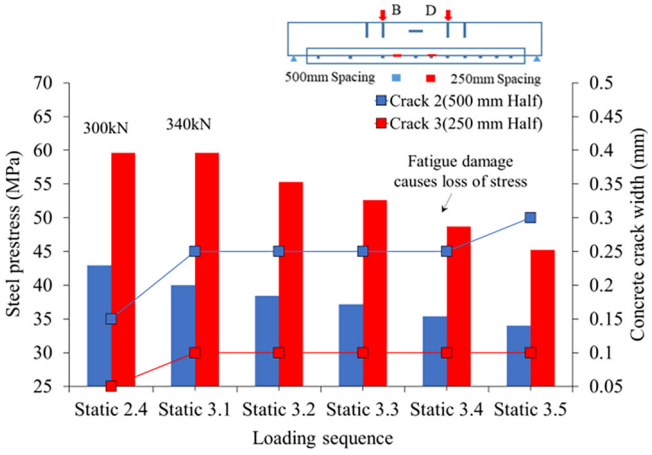

Fig. 21. Steel lower flange prestress in stage 3.

D, and at 40 MPa in section B, prestress decreased to 45 MPa and 35 MPa, respectively, as concrete cracks got deeper, and crack width increased to 0.3 mm in crack 2 by the end of this stage. Steel-lower-flange prestress in section B being 34 MPa with loss of 43%, compared to 45 MPa in section D with loss of 25%, made

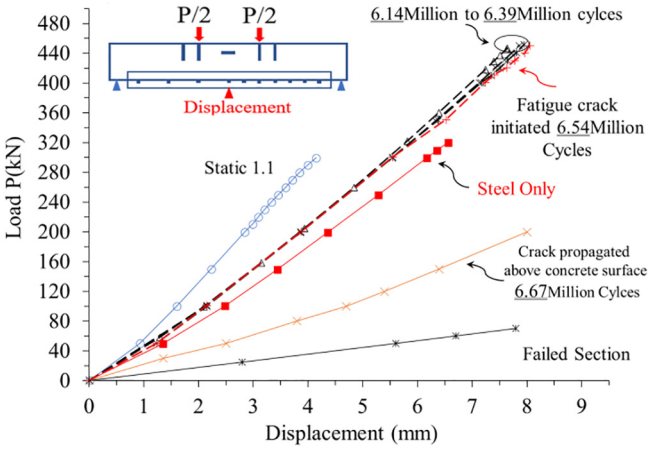

Fig. 22. Load and displacement relationship.

the two halves of the girder different due to concrete crack width being remarkably larger in the prior half.

As the section went through larger stress ranges in steel-lower-flange, concrete cracks got deeper, and crack width increased, the neutral axis location was changed, and steel lower flange prestress was decreased. However, the load and displacement relationship did not reflect any remarkable changes.

3.3. Structural performance after crack initiation in steel-lower-flange

To study the behavior of the specimen after crack initiation in steel-lower-flange, after static 3.5 (6,140,000 cycles) the specimen was cyclically loaded with a load range of 440 kN (10–450 kN) that caused stress ranges about 126 MPa in steel-lower-flange. At 6,540,000 cycles, with a sudden drop of steel-lower-flange stress, fatigue crack initiated in the shear rib weld joint in section D in the 250-mm half. Further cyclic loading caused the propagation of steel fatigue crack to about 150 mm above the concrete upper surface.

Concrete crack width increased to 0.4 mm in crack 2 in the 500-mm half at 6,240,000 cycles and remained the same until 6,390,000 cycles, while crack 3 in the 250-mm half remained with the same width of 0.1 mm. At 6,540,000 cycles, initiation of fatigue crack in section D, resulted in the width of concrete crack 3 increased to 0.3 mm, and the width of crack 4 right under the failed shear rib at section D increased to 0.4 mm, same as crack 2 in the opposite half.

Load and displacement relationship in this loading stage, as shown in Fig. 22, did not show any change in the midspan displacement even after fatigue crack initiated in steel-lower-flange. The change was remarkable after the fatigue crack propagated above the concrete surface at 6,670,000 cycles.

Steel-lower-flange nominal stress and prestress shown in Figs. 23 and 24, respectively, illustrated remarkable change in section D after fatigue crack initiation under 6,540,000 cycles. However, values in section B changed after the fatigue crack in section D propagated above concrete surface at 6,670,000 cycles.

Finally, the specimen was statically displaced to 70 mm at midspan to take it to its ultimate failure, shown in Fig. 25. Investigation of the failed shear rib in section D, showed that the shear rib failed due to overlap weld defect, not due to the shear rib weld joint reaching its fatigue capacity.

Even though the load and displacement relationship did not change after steel-lower-flange crack initiation, and concrete crack width advancing to 0.4 mm, steel-lower-flange nominal stress and prestress remarkably changed after crack initiation. This again

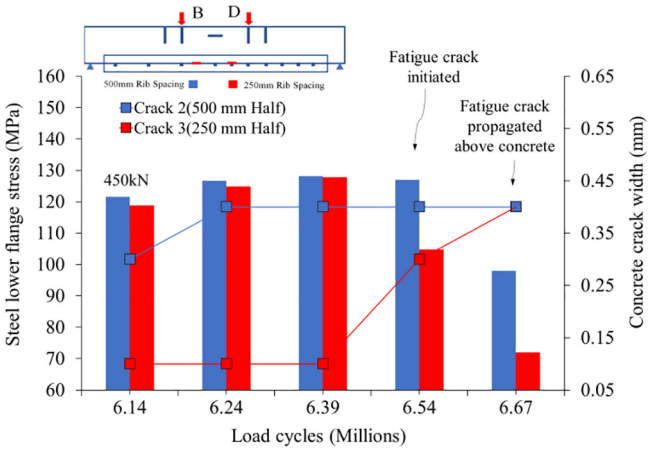

Fig. 23. Steel lower flange nominal stress.

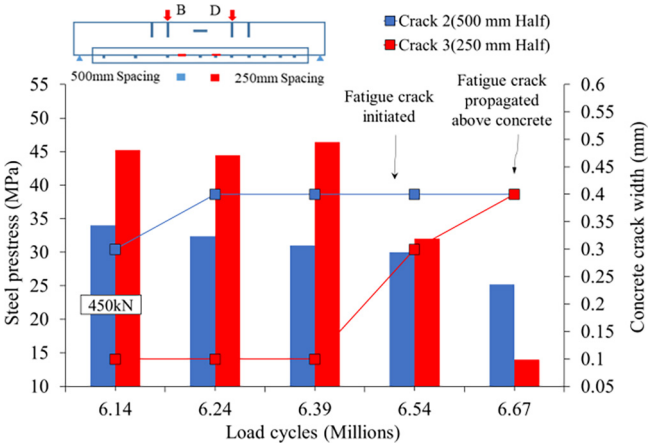

Fig. 24. Steel lower flange prestress.

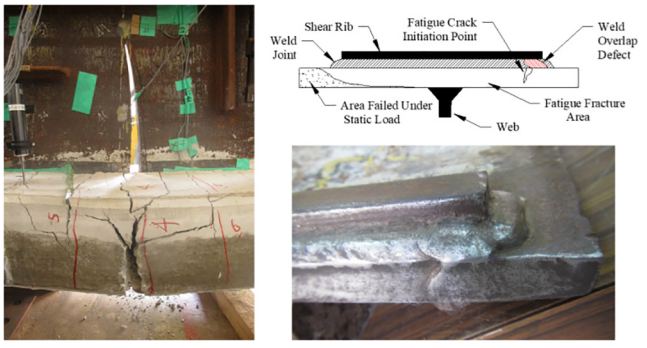

Fig. 25. Shear rib failure in section D.

confirms that the load and displacement relationship does not relate to changes in sectional properties. However, changes in the load and displacement relationship appeared very late after the fatigue crack already propagated above the concrete surface, which is very late and cannot be helpful for monitoring approaches.

4. Monitoring recommendations

The trend of changes born by the preflex beam section as concrete deteriorates under cyclic loading, shows that the concrete crack width as an important monitoring factor utilized for monitoring purpose, relate very well to the changes occurring in the preflex beam. This study, with its scope being in experimental research-level outlines the followings to be considered in monitoring and maintenance approaches for the preflex beams:

- Concrete crack widths of up to 0.1 mm that are usually expected soon after initial concrete cracking takes place (stage one of this study) does not cause remarkable loss of prestress in steel lower flange. Consequently, no remarkable changes in sectional properties are expected.
- Crack widths larger than 0.1 mm up to 0.2 mm (stage two), or in other words, an increase of crack width up to two times of that in initial cracking stage, would mean that steel-lower-flange prestress, and consequently sectional properties of preflex beam, have already started undergoing changes and will further change under repetitive loadings. Maintenance measures should be employed to make sure the preflex beam does not deteriorate further.
- If concrete crack width is larger than 0.2 mm up to 0.3 mm (stage three), or about three times of the crack width in initial cracking stage, that is expected when steel-lower-flangeis bearing stress ranges accumulating fatigue damage in steel-lower-flange, major loss of prestress in steel-lower-flange and remarkable changes in sectional properties are expected. Proper maintenance measures are required to make sure steel-lower-flange has not reached or is not about to reach fatigue damage capacity.
- Crack widths larger than 0.3 mm that will be about four times of that in initial cracking stage would mean that steel-lower-flange weld joint is expected or already have developed fatigue crack, and remarkable changes challenging serviceability of the structure have been born by the preflex beam bridge.
- Even if the preflex beam goes through severe deterioration in lower-flange concrete that in turn leads to loss of steel prestress and change in sectional properties, the load and displacement relationship will not be reflecting the changes born by the section leading to an underestimated evaluation of the state of preflex beam.
- Closer spacing of shear ribs welded to the steel-lower-flange keeps the width of the concrete cracks small under cyclic loading, that helps in minimizing loss of steel prestress and thus changes in sectional properties that are key for a durable girder. The number of concrete cracks will be more though with the closer spacing of shear ribs.

This study has experimentally addressed behavior of preflex beam under cyclic loading and the changes in structural behavior of the beam. Use of Finite Element Modelling (FEM) and other numerical methods as possible ways for validation of experimental results and further clarification of preflex beam's behavior under cyclic loading, will be an important and remarkable contribution to relevant literature.

5. Conclusion

As a typical procedure utilized for inspection and monitoring of actual preflex beam bridges, firstly, concrete cracking, efflorescence, and spalling, and then displacement and stiffness, are assessed through detailed testing and survey based on which evaluation of preflex beam girder is carried out. In this study, changes in the sectional properties and prestress, resulted due to concrete aging deterioration of the preflex beam girder are clarified, and then recommendations to be considered for monitoring and maintenance approaches are outlined. The conclusions are shown below:

- Changes in load and displacement relationship do not depict the changes that occur in the mechanical properties of the section and loss of steel-lower-flange prestress, knowledge of which is very important to fairly evaluate the service state of the preflex beam. In other words, no or slight changes in load and displacement relationship can be accompanied by remarkable changes in sectional properties and loss of prestress. This phenomenon suggests not solely relying on load and displacement relationships to evaluate the service state of the preflex beam girder.
- Changes in the concrete crack width can very well relate to the state of steel-lower-flange prestress and the changes in sectional properties of the preflex beam, and therefore can give a reliable evaluation of the state of preflex beam girder. Therefore, concrete crack width shall be considered as an important index to evaluate changes in the girder rather than load and displacement relationship, to make sure changes happening in the sectional properties of preflex beams are not underestimated.

Declaration of Competing Interest

The authors declare that they have no known competing financial interests or personal relationships that could have appeared to influence the work reported in this paper.

References

[1] S. Staquet, G. Rigot, H. Detandt, B. Espion, Innovative composite precast prestressed precambered U-shaped concrete deck for Belgium's high speed railway trains, PCI J. 46 (2004) 94–113.
[2] Z.B. Pap, PREFLEX girders: Prefabricated composite bridges. Bauhaus Summer School in Forecast Engineering, Weimar, Germany, 2014.
[3] I. Maruyama, O. Kontani, M. Takizawa, S. Sawada, S. Ishikawao, J. Yasukouchi, O. Sato, J. Etoh, T. Igari, Development of soundness assessment procedure for concrete members affected by neutron and gamma-ray irradiation, J. Adv. Concr. Technol. 15 (9) (2017) 440–523.
[4] H. Kabir, R.D. Hooton, N.J. Popoff, Evaluation of cement soundness using the ASTM C151 autoclave expansion test, Cem. Concr. Res. 136 (2020) 106159.
[5] G. Portela, U. Barajas, Albarran-Garcia, J.A. Analysis and load rating of Pre-flex composite beams, 2011.
[6] D. Bae, K.M. Lee, Behavior of preflex beam in manufacturing process, KSCE J. Civ. Eng. 8 (2004) 111–115.
[7] H. Watanabe, Y. Takeda, T. Tsutsumishita, A. Kurita, S. Matsui, New fabrication methods for long span preflexed beam and its constructed examples, in: Proc. of the 3rd Int. Conf. on Steel-Concrete Composite Structures ASCCSS, 1991, pp. 569–574.
[8] S.G. Morano, C. Mannini, Preflex beams: a method of calculation of creep and shrinkage effects, J. Bridge Eng. 11 (2006) 48–58.
[9] Mannini, C., Morano, S.G., Preflex beams: Structural optimization and analysis of economic advantages, Advances in Bridge Maintenance, Safety Management, and Life-Cycle Performance, Set of Book & CD-ROM, pp. 875-876, 2015.
[10] L. Wan, Q. Gao, Study on the bending behavior of preflex beam, AIP Conf. Proc. 1864 (1) (2017) 020108.
[11] S. Kiuchi, Destructive test of preflex beam, Bulletin of Faculty of Engineering, Kanazawa University 5 (3) (1969) 193–204 (In Japanese).
[12] S.J. Errera, C.P. Pitts, D.W. Haines, Tests of preflexed beams, Fritz Engineering Laboratory Report No. 282.1, 1961.
[13] F.A. Mink, An experimental investigation of the 'preflex' method of prestressing concrete, Doctoral dissertation, Georgia Institute of Technology (1955).
[14] K. Zhang, S. Li, K. Liu, Experimental Study on Static and fatigue behavior of steel-concrete preflex prestressed composite beam, Advances in Steel Structures (ICASS99) ICASS99 (1999) 965–973.
[15] H. Kikuchi, H. Abe, H. Watanabe, Fatigue test of preflexed beam, PREBEAM, Prebeam promotion society 10th anniversary, pp. 219-22, 1981. (In Japanese).
[16] K. Yasuhiro, T. Tsutsumishita, Fatigue strength test of welded dowel bars in preflex composite girder, The 45th annual scientific lecture meeting of the Japan Society of Civil Engineers, 1990. (In Japanese).
[17] A. Hobbacher, "IIW Recommendations for Fatigue Design of Welded Joints and Components, Revised September 2013., IIW-doc." (2013): 2460-13.